This is the peer reviewd version of the followng article:

Mid IR hollow core fiber gas laser emitting at 4.6 μm / Aghbolagh, F.B.A., Nampoothiri, V., Debord, B., Gerome, F., Vincetti, L., Benabid, F., Rudolph, W.. - In: OPTICS LETTERS. - ISSN 0146-9592. - 44:2(2019), pp. 383-386. [10.1364/OL.44.000383]

Terms of use:

The terms and conditions for the reuse of this version of the manuscript are specified in the publishing policy. For all terms of use and more information see the publisher's website.

24/11/2026 20:41

(Article begins on next page)

OSA
The Optical Society

Accepted Author Manuscript

Journal:	*Optics Letters*
Article Title:	Mid IR hollow core fiber gas laser emitting at 4.6 μm
Authors:	F. B. A. Aghbolagh, V. Nampoothiri, B. Debord, F. Gerome, L. Vincetti, F. Benabid, and W. Rudolph
Accepted for publication:	07 December 2018
Final version published:	11 January 2019
DOI:	https://doi.org/10.1364/OL.44.000383

Access to this article is made available via CHORUS and subject to OSA Publishing Terms of Use.

Mid IR hollow core fiber gas laser emitting at 4.6 μm

F. B. A. AGHBOLAGH,[1,*] V. NAMPOOTHIRI,[1] B. DEBORD,[2] F. GEROME,[2] L. VINCETTI,[3] F. BENABID,[2] W. RUDOLPH[1]

[1]Department of Physics and Astronomy, University of New Mexico, Albuquerque, NM 87131, USA
[2] GPPMM group, Xlim Research Institute, UMR CNRS 7252, Université de Limoges, France
[3] Dept. of Engineering "Enzo Ferrari", University of Modena and Reggio Emilia, Italy
*Corresponding author: F. B. A. Aghbolagh_farzinbeygiazar2020@unm.edu

Received XX Month XXXX; revised XX Month, XXXX; accepted XX Month XXXX; posted XX Month XXXX (Doc. ID XXXXX); published XX Month XXXX

Emission at 4.6 μm was observed from an N_2O filled hollow core fiber laser. 8-ns pump pulses at 1.517 μm excited a vibrational overtone resulting in lasing on an R and P branch fundamental transition from the upper pump state. At optimum gas pressure of 80 Torr a photon conversion efficiency of 9% and a slope efficiency of 3% was observed from a mirrorless laser. The laser threshold occurred at an absorbed pump energy of 150 nJ in a 45-cm long fiber with 85 μm core diameter. The observed dependence of the laser output on gas pressure is shown to be a result of line broadening and relaxation rates.

© 2018 Optical Society of America

OCIS codes: *(140.3510) Lasers, fiber; (140-1340) Atomic gas lasers; (140.3070) Infrared and far-infrared lasers; (060.2310) Fiber optics.*

http://dx.doi.org/10.1364/OL.99.099999

Infrared laser sources emitting in the 3-5 μm and 8-13 μm atmospheric transmission window are attractive for applications such as remote sensing, imaging and free-space communications [1]. Extension of the emission wavelength of silica-based solid core fiber lasers into the IR spectral region is problematic because of absorption losses of the host materials. The advent of hollow core photonic crystal fibers (HCPCFs) [2] and the possibility to fill them with gases opened new avenues for laser development and nonlinear optics [3], taking advantage of the long interaction length of the interacting fields and their small modal areas. Within this context, the HCPCFs that guide via Inhibited Coupling (IC) [4] are attractive because they exhibit a guided field that overlaps weakly with the glass cladding material. The optical overlap factors η, which can range from 10^{-4} to 10^{-6} [5], are lower than those of index guiding solid core fibers or photonic bandgap HCPCFs. Consequently, material absorption losses are modest up to the mid infrared region for a few meter long IC guiding HCPCFs made from silica. HCPCFs have already been demonstrated to guide beyond the 4 μm region where bulk fused silica becomes opaque [6,7].

For lasers, the useable transmission region can be expected to extend into the IR as long as the gain exceeds the propagation loss (per unit length), which is possible with gas active media. Gas filled HCPCFs have the guiding properties of photonic crystal structures while pushing the onset of detrimental nonlinear optical processes to higher intensities compared with solid core fibers [8,9]. Gas filled HCPCFs were reported first as both pulsed [10] and CW [11] Raman lasers, and later as pulsed systems based on population inversion in C_2H_2 [12]. The latter concept, hollow fiber gas laser (HOFGLAS), was also demonstrated as CW laser in the VIS with I_2 [13,14] and NIR with C_2H_2 [15]. A HCPCF filled with molecular hydrogen extended the output wavelength of a Raman laser to 4.4 μm [16].

Depending on the gas and spectral region of interest, the pump and gain transitions in HOFGLAS can involve electronic, vibrational and rotational states and combinations thereof. Transition cross sections range from $>10^{-14}$ cm^2 for fundamental, dipole allowed electronic transitions to $< 10^{-21}$ cm^2 for excitation of vibrational overtones where the change of the vibrational quantum number $\Delta v \geq 2$. The optical depth can be controlled by the gas pressure and fiber length. Compared to dopants in solid core fibers gases have much narrower line widths. However, the multitude of rotational levels provides the possibility of lasing at discrete wavelengths.

In this letter we report on an optically pumped N_2O filled hollow core fiber laser pumped on a second overtone transition at 1.517 μm, which resulted in emission from a fundamental ro-vibrational transition ($3v_3$ to $2v_3$) at 4.6 μm. Lasing at 4.6 μm of N_2O in a regular gas cell was achieved previously by using an OPO pump source at 2.88 μm [17]. Our system extends the output of HOFGLAS to the 4-5 μm region. An energy level diagram of N_2O with the relevant transitions is shown in Fig.1.

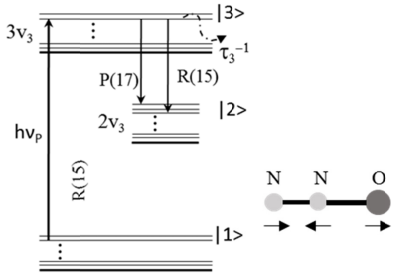


Fig.1. Simplified energy diagram of N_2O showing three vibrational bands belonging to the N-O stretch mode v_3. The pump excites the second overtone.

Figure 2 compares the transmission behavior of bulk fused silica (solid data points) and an IC guiding HCPCF with 85 μm inner core diameter. The fiber distinguishes itself by its ultra-broad

transmission windows and an extremely small optical overlap of its core mode HE_{11} with the silica cladding. The latter property allows optical guidance in wavelength regions where the glass strongly absorbs.

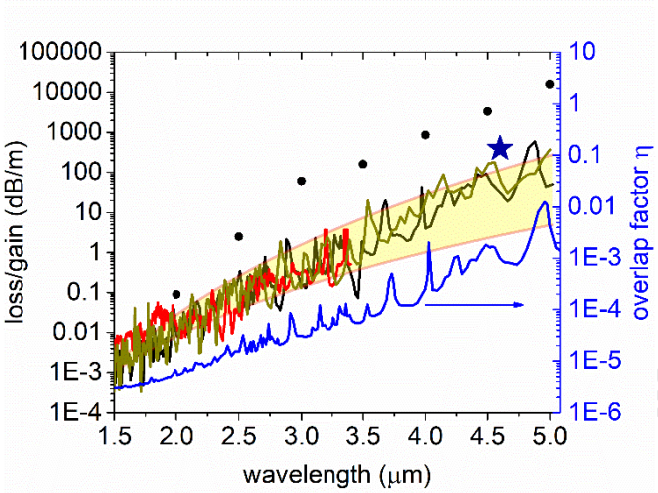


Fig. 2. Loss coefficient α_m versus wavelength for bulk fused silica (solid circle, data from Heraeus Suprasil 300 [18]). Measured loss in the HCPCF used for our HOFGLAS (red solid line). Numerically calculated confinement loss of the HCPCF core-fundamental mode in the case of a glass material with no absorption (black solid line), and when material absorption is taken into account (dark-cyan solid line). The shaded region is a guide for the eye of the transmission loss range. The star symbol corresponds to the calculated gain coefficient of N_2O at 4.6 μm, see text. The blue solid curve shows the calculated optical overlap of the fiber core fundamental mode.

The fiber exhibits a Kagome-lattice cladding and a hypocycloid (i.e. negative curvature) core-contour to enhance the IC and thus reducing the fiber confinement loss [19,20]. The fiber has an outer diameter of 300 μm, an inner core diameter of 85 μm, silica strut thickness of 490 nm, and a negative curvature parameter $b \approx 0.4$. The measured loss spectrum is shown from 1.5 μm to 3.4 μm (red solid line). At the pump wavelength (1.517 μm) the fiber loss is about 30 dB/km. The figure shows the calculated confinement loss (CL) of the core fundamental mode of the HCPCF over the wavelength range from 1.5 μm to 5 μm when the glass material absorption is neglected (black solid line) and absorption is taken into account (dark-cyan). The fused silica absorption coefficient $\alpha_m(\lambda)$ is obtained by interpolating the data points (solid circles) in Fig.2. The CL can also be estimated qualitatively from simple scaling laws reported in [21]. The calculated CL and the measured loss show a good agreement with the experimental data over the measured spectral range. For an overlap factor $\eta << 1$, the effective propagation loss coefficient can be estimated with the sum $\alpha_{eff} \approx \alpha_{CL} + \alpha_m\eta$, where α_{CL} is CL loss for the case of a non-absorbing material. Here, we ignore the loss due to surface scattering [5]. Figure 2 shows that the contribution of the material absorption to the propagation loss is ~3.6 dB/m, yielding an effective propagation loss of $\alpha_{eff} \approx 33.6$ dB/m. This loss figure is qualitatively in agreement with the numerically calculated CL of ~55 dB/m with absorption included. The calculated N_2O gain is about five times larger, cf. Fig.2.

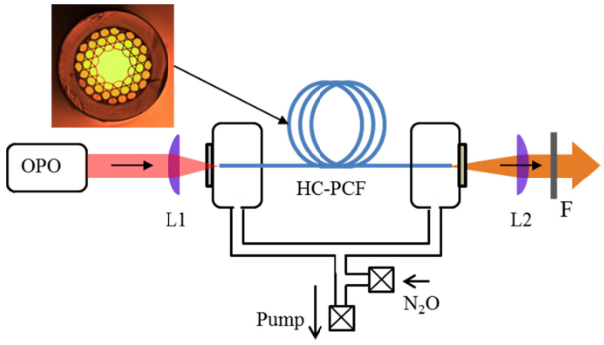


Fig. 3. Experimental setup of the 4.6 μm pulsed N_2O laser. The inset shows the cross section of the 45-cm long fiber. The pump was an 8-ns pulse at 1.517 μm from an OPO. To control the pressure the two ends of the fiber were housed in small chambers. "F" denotes a long pass germanium filter used to block residual pump radiation.

The experimental setup of the laser is shown in Fig.3. Pulses from an 8-ns OPO at 1.517 μm are coupled into a 45-cm long Kagome HCPCF using an uncoated CaF_2 lens with a focal length of 5-cm. The coupling efficiency was about 45%. The output is monitored with a spectrometer and a HgCdTe energy meter.

Lasing is observed without an external cavity. As reported with other HOFGLASs, the gain is large enough to produce laser-like output based on amplified spontaneous emission. The laser spectrum is shown in Fig.4. The two spectral lines of the laser emission belong to the P(17) and R(15) transition, originating at the upper pump level, see Fig.1.

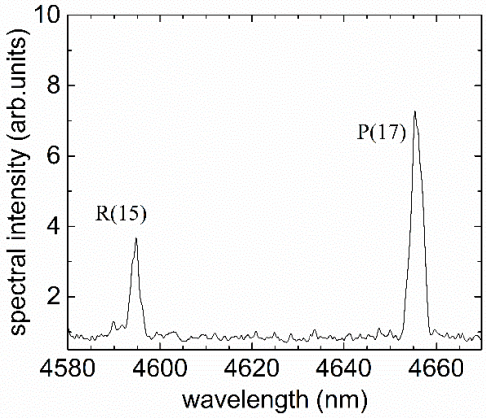


Fig. 4. Measured spectrum of the N_2O laser. Details of the lines are not resolved. p = 80 Torr, absorbed pump energy E_{abs} = 1.3 μJ.

Figure 5 shows the measured laser output as a function of the gas pressure. Maximum output was observed at a pressure of $p_{opt} \approx 80$ Torr. Figure 6 shows the laser pulse energy as a function of the absorbed pump pulse energy. At optimum pressure the slope efficiency was 3%. The threshold occurred at an absorbed pump pulse energy of about 150 nJ.

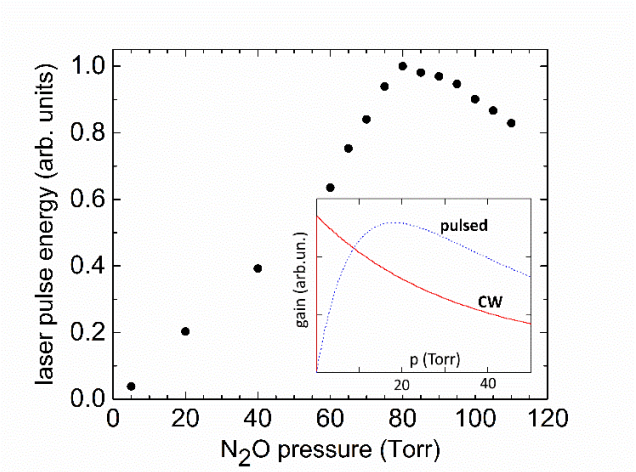


Fig. 5. Measured laser output as a function of N_2O pressure for 70 µJ of pump energy coupled into fiber. The inset shows the calculated gain coefficient $g_{32}(p)$, see text.

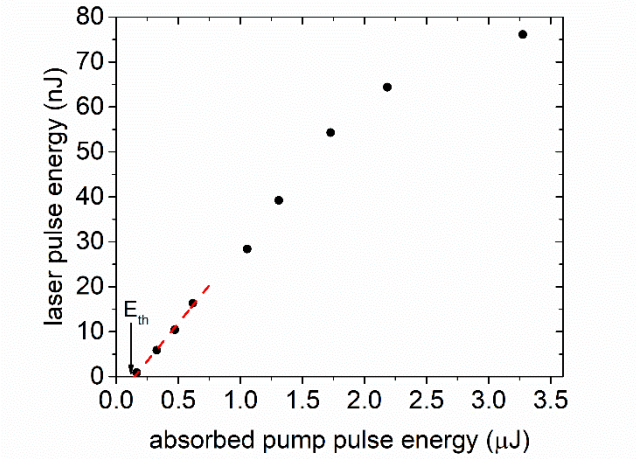


Fig. 6. Laser pulse energy as a function of absorbed pump pulse energy for a 45-cm long fiber filled with 80 Torr of N_2O gas. The intersection of the dashed line with the "x" axis marks the experimentally determined threshold $E_{th} \approx 0.150$ µJ.

For an estimation of the gain and its pressure dependence we refer to the energy level scheme shown in Fig.1. For simplicity we will consider only one of the two possible gain transitions. To obtain lasing without feedback from a cavity the gain has to exceed the losses in each segment of the fiber if we assume constant pump intensity and neglect saturation. To obtain the gain coefficient we first calculate the number density of molecules excited to the upper laser level, N_3, if the pump (intensity I_p) is turned on at $t = 0$ and obtain:

$$N_3(t) = \frac{\sigma_{13} N_1}{h\nu_p} I_p \tau_3 \left(1 - e^{-t/\tau_3}\right) \quad \textbf{(1)}$$

Here σ_{13} is the absorption cross section, N_1 is the number density of molecules in the rotational state (J = 15) of the vibrational ground state that absorbs the pump, and $1/\tau_3$ is the total removal rate of molecules from the excited rotational state, see Fig.1. The small signal gain coefficient

$$g_{32} = \sigma_{32} N_3, \quad \textbf{(2)}$$

with σ_{32} being the gain cross section. We omitted a factor of approximately ½ that takes into account gain sharing between the R and P transition. For pulse durations $\tau_p >> \tau_3$ and CW excitation, $g_{32} \approx \sigma_{32}\sigma_{13} N_1 I_p \tau_3 / h\nu_p$, and for $\tau_p << \tau_3$ the maximum gain coefficient reached at the end of the pulse $g_{32} \approx \sigma_{32}\sigma_{13} N_1 I_p \tau_p / h\nu_p$. These expressions were obtained after simplifying the term in brackets in Eq. (1). The second-overtone absorption cross section σ_{13} for N_2O is about 10^{-20} cm^2. A typical emission cross section for a fundamental ro-vib transition in N_2O is 10^{-15} cm^2 [22]. At 300 K, about 4% of the N_2O molecules occupy the lower pump state. The relaxation time $\tau_3 = R/p$ with $R \approx 10^{-7}$ sTorr [23] as a typical value at room temperature for rotational relaxation. Thus, for a gas pressure of p = 80 Torr and a 40 µJ pump pulse propagating in a HCPCF with 85 µm inner core diameter, $\tau_3 \approx 1.3$ ns and $N_3 \approx 9 \times 10^{14}$ cm^{-3}. Equation (2) then yields a gain coefficient of $g_{32} \approx 0.9$ cm^{-1}, which is shown in Fig. 2 (in dB/m).

As long as the fiber loss coefficient $\alpha_{eff} < g_{32}$, spontaneously emitted light will be amplified. If the overall gain is large enough the radiation at the fiber end is spectrally narrowed with properties similar to a laser with external cavity. The relatively large gain coefficient suggests that HOFGLAS can extend even further into the IR, see Fig.2.

In HOFGLAS, the gas pressure is an important adjustment parameter for optimizing the laser output [9]. This results from the pressure dependence of the gas parameters that enter the expression for the gain; – transition line width $\Delta\nu$, cross sections $\sigma \propto 1/\Delta\nu$, relaxation rates $\tau_3 \propto R/p$ and number density in the ground state N_1. In the pressure and temperature range of interest, the transitions are affected by Doppler and collisional broadening and the width of the resulting Voigt profile can be approximated by $\Delta\nu(p) \approx 0.53\beta p + \sqrt{0.217\beta^2 p^2 + \Delta\nu_D^2}$ [24], where β is the pressure broadening coefficient for self-collisions, and $\Delta\nu_D$ is the Doppler linewidth. For an estimation we use $\beta \approx 8$ MHz/Torr [22] for both absorption and gain transition and $\Delta\nu_D$ = 100 MHz, 370 MHz for the gain and absorption transition, respectively. The pressure dependence $g_{32}(p)$ can now be evaluated with the help of Eqs. (1) and (2) and is shown as inset in Fig.5 for a CW pump and an 8-ns pump pulse.

In both cases there is an optimum pressure that maximizes $g(p)$ for given input pump intensity. The optimum pressure value for CW is in the sub Torr region as observed in Ref. [25]. The reason is the fast removal rate from the excited state, $1/\tau_3$ for these conditions. For the pulsed case, the calculated optimum pressure p_{opt} is lower than what we observed, 18 Torr versus 80 Torr. The discrepancy is due to a number of factors. First, the spectral width of our pump pulse $\Delta\nu_p \sim 3$ GHz, which leads to an increase in absorption with increasing pressure until about $p \approx 350$ Torr at which $\Delta\nu \sim \Delta\nu_p$. Second, the laser output is

affected by saturation of the laser transition, which is neglected in the estimation for the small signal gain. A fast relaxation out of the lower laser level is beneficial for efficiency. This favors a larger pressure and is expected to increase p_{opt}.

In summary, we have demonstrated an N_2O HOFGLAS in the mid-infrared spectral region optically pumped on a second overtone. The achieved slope efficiency at optimum pressure of 80 Torr was 3%. No attempt was made to optimize the laser output by finding the optimal fiber length and other parameters. Optimization of these parameters is likely to result in higher slope efficiency. The observed emission wavelength of 4.6 μm and our gain estimations suggest the potential of silica based HOFGLASs to extend laser emission beyond 5 μm with gases as active medium.

Funding. Air Force Research Lab (FA9451-17-2-0011), College of Arts and Sciences at the University of New Mexico (UNM).

Acknowledgment. We are grateful for the loan of a diode laser under the Education Partnership Agreement (EPA) 2011-AFRL/RD&RV-EPA-01 between the Air Force Research Laboratory and the University of New Mexico. We thank L. Emmert (UNM), and K. Corwin and B. Washburn (Kansas State University) for helpful discussions.

References

1. S. D. Jackson, Nature Photonics **6,** 423 (2012).
2. R. F. Cregan, B. J. Mangan, J. C. Knight, T. A. Birks, P. S. J. Russell, P. J Roberts, and D. C. Allan, Science. **285,** 1537 (1999).
3. A. R. Bhagwat, and A. L. Gaeta, Optics Express **16,** 5035 (2008).
4. F. Couny , F. Benabid, P. J. Roberts, P. S. Light, and M. G. Raymer, Science. **318,** 1118 (2007).
5. B. Debord, A. Amsanpally, M. Chafer, A. Baz, M. Maurel, J. M. Blondy, E. Hugonnot, F. Scol, L. Vincetti, F. Gérôme, and F. Benabid, Optica **4,** 209 (2017).
6. A. N. Kolyadin, A. F. Kosolapov, A. D. Pryamikov, A. S. Biriukov, V. G. Plotnichenko, and E. M. Dianov, Optics Express. **21,** 9514 (2013).
7. A. D. Pryamikov, A. S. Biriukov, A. F. Kosolapov, V. G. Plotnichenko, S. L. Semjonov, and E. M. Dianov, Optics Express. **19,** 1441 (2011).
8. J. W. Dawson, M. J. Messerly, R. J. Beach, M. Y. Shverdin, E. A. Stappaerts, A. K. Sridharan, P. H. Pax, J. E. Heebner, C. W. Siders, and C. P. J. Barty, Opt. Express. **16,** 13240 (2008).
9. A. V. V. Nampoothiri, A. M. Jones, C. Fourcade-Dutin, C. Mao, N. Dadashzadeh, B. Baumgart, Y. Y. Wang, M. Alharbi, T. Bradley, N. Campbell, F. Benabid, B. R. Washburn, K. L. Corwin, and W. Rudolph, Opt. Mater. Express. **2,** 948 (2012).
10. F. Benabid, J. C. Knight, G. Antonopoulos, and P. St. J. Russell, Science. **298,** 399 (2002).
11. F. Couny, F. Benabid, and P.S. Light, Phys Rev Lett. **99,** 143903-1 (2007).
12. A. M. Jones, A. V. V. Nampoothiri, A. Ratanavis, T. Fiedler, N. V. Wheeler, F. Couny, R. Kadel, F. Benabid, B. R. Washburn, K. L. Corwin, and W. Rudolph, Optics Express. **19,** 2309 (2011).
13. A. V. V. Nampoothiri, B. Debord, M. Alharbi, F. Gérôme, F. Benabid, and W. Rudolph, Opt. Lett. **40,** 605 (2015).
14. A. V. V. Nampoothiri, F. B. A. Aghbolagh, B. Debord, F. Gerome, F. Benabid, and W. Rudolph, Appl. Opt. **56,** 9592 (2017).
15. M. R. A. Hassan, F. Yu, W. J. Wadsworth, and J. C. Knight, Optica. **3,** 218 (2016).
16. A. V. Gladyshev, A. F. Kosolapov, M. M. Khudyakov, Yu. P. Yatsenko, A. N. Kolyadin, A. A. Krylov, A. D. Pryamikov, A. S. Biriukov, M. E. Likhachev, I. A. Bufetov and E. M. Dianov, Quantum Electronics **47,** 491 (2017).
17. H. C. Tapalian, C. A. Michaels, and G. W. Flynn, Appl. Phys. Lett. **70,** (1997).
18. https://www.heraeus.com/en/hqs/fused_silica_quartz_knowledge_base/knowledge_overview/knowlegde_intro.aspx
19. Y. Y. Wang, N. V. Wheeler, F. Couny, P. J. Roberts, and F. Benabid, Opt. Lett. **36,** 669 (2011).
20. B. Debord, M. Alharbi, T. Bradley, C. Fourcade-Dutin, Y.Y. Wang, L. Vincetti, F. Gérôme, and F. Benabid, Optics Express. **21,** 28597 (2013).
21. M. Maurel, M. Chafer, A. Amsanpally, M. Anan, F. Amrani, B. Debord, L. Vincetti, F. Gerome, and F. Benabid, Opt. Lett. **43,** 1598 (2018).
22. HITRAN database, http://cfa-www.harvard.edu/HITRAN/
23. S. P. Phipps, T. C. Smith, G. D. Hager, M. C. Heaven, J. K. McIver, and W. Rudolph, Journal of Chem. Phys. **116,** 9281 (2002).
24. J. J. Olivero, and R. L. Longbothum, Journal of Quantitative Spectroscopy and Radiative Transfer. **17,** 233 (1977).
25. M. Xu, F. Yu, and J. Knight, Opt. Lett. **42,** 4055 (2017).

Full References

1. S. D. Jackson, "Towards high-power mid-infrared emission from a fiber laser," Nature Photonics **6**, pp. 423-431 (2012).
2. R. F. Cregan, B. J. Mangan, J. C. Knight, T. A. Birks, P. S. J. Russell, P. J Roberts. and D. C. Allan, "Single-mode photonic band gap guidance of light in air," Science. **285**, pp.1537-1539 (1999).
3. A. R. Bhagwat, and A. L. Gaeta, "Nonlinear optics in hollow-core photonic bandgap fibers, " Optics Express **16** (7), pp. 5035-5047 (2008).
4. F. Couny , F. Benabid, P. J. Roberts, P. S. Light, and M. G. Raymer, "Generation and photonic guidance of multi-octave optical frequency combs," Science. **318** (5853)**,** pp. 1118-1121 (2007).
5. B. Debord, A. Amsanpally, M. Chafer, A. Baz, M. Maurel, J. M. Blondy, E. Hugonnot, F. Scol, L. Vincetti, F. Gérôme, and F. Benabid, " Ultralow transmission loss in inhibited-coupling guiding hollow fibers, " Optica **4** (2), pp. 209-217 (2017).
6. A. N. Kolyadin, A. F. Kosolapov, A. D. Pryamikov, A. S. Biriukov, V. G. Plotnichenko, and E. M. Dianov, "Light transmission in negative curvature hollow core fiber in extremely high material loss region," Optics Express. **21** (8), pp.9514-9519 (2013).
7. A. D. Pryamikov, A. S. Biriukov, A. F. Kosolapov, V. G. Plotnichenko, S. L. Semjonov, and E. M. Dianov, "Demonstration of a waveguide regime for a silica hollow - core microstructured optical fiber with a negative curvature of the core boundary in the spectral region > 3.5 μm," Optics Express. **19** (2), pp. 1441-1448 (2011).
8. J. W. Dawson, M. J. Messerly, R. J. Beach, M. Y. Shverdin, E. A. Stappaerts, A. K. Sridharan, P. H. Pax, J. E. Heebner, C. W. Siders, and C.P.J. Barty, "Analysis of the scalability of diffraction-limited fiber lasers and amplifiers to high average power," Opt. Express. **16** (17), pp. 13240-13266 (2008).
9. A. V. V. Nampoothiri, A. M. Jones, C. Fourcade-Dutin, C. Mao, N. Dadashzadeh, B. Baumgart, Y.Y. Wang, M. Alharbi, T. Bradley, N. Campbell, F. Benabid, B. R. Washburn, K. L. Corwin, and W. Rudolph, "Hollow-core Optical Fiber Gas Lasers (HOFGLAS): a review [Invited]," Opt. Mater. Express. **2** (7), pp. 948-961 (2012).
10. F. Benabid, J. C. Knight, G. Antonopoulos, and P. St. J. Russell, " Stimulated Raman Scattering in Hydrogen-Filled Hollow-Core Photonic Crystal Fiber," Science. **298** (5592), pp. 399-402 (2002).
11. F. Couny, F. Benabid, and P.S. Light, "Subwatt Threshold cw Raman Fiber-Gas Laser Based on H_2-Filled Hollow-Core Photonic Crystal Fiber," Phys Rev Lett. **99** (14), pp. 143903-1-143903-4 (2007).
12. A. M. Jones, A. V. V. Nampoothiri, A. Ratanavis, T. Fiedler, N. V. Wheeler, F. Couny, R. Kadel, F. Benabid, B. R. Washburn, K. L. Corwin, and W. Rudolph, "Mid-infrared gas filled photonic crystal fiber laser

based on population inversion," Optics Express **19** (3), pp.2309-2316 (2011).
13. A. V. V. Nampoothiri, B. Debord, M. Alharbi, F. Gérôme, F. Benabid, and W. Rudolph, "CW hollow-core optically pumped I_2 fiber gas laser," Opt. Lett. **40** (4), pp. 605-608 (2015).
14. A. V. V. Nampoothiri, F. B. A. Aghbolagh, B. Debord, F. Gerome, F. Benabid, and W. Rudolph, "High photon conversion efficiency continuous wave lasing in an optically pumped I_2 hollow fiber gas laser in the visible region," Appl. Opt. **56** (34), pp. 9592-9595 (2017).
15. M. R. A. Hassan, F. Yu, W. J. Wadsworth, and J. C. Knight, " Cavity-based mid-IR fiber gas laser pumped by a diode laser, " Optica. **3** (3), pp. 218-221 (2016).
16. A. V. Gladyshev, A. F. Kosolapov, M. M. Khudyakov, Yu. P. Yatsenko, A. N. Kolyadin, A. A. Krylov, A. D. Pryamikov, A. S. Biriukov, M. E. Likhachev, I. A. Bufetov and E. M. Dianov, "4.4-μm Raman laser based on hollow-core silica fiber," Quantum Electronics **47** (5), pp. 491-494 (2017).
17. H. C. Tapalian, C. A. Michaels, and G. W. Flynn, "Mid infrared molecular gas lasers optically pumped by a continuously tunable infrared optical parametric oscillator," Appl. Phys. Lett. **70** (17), (1997).
18. https://www.heraeus.com/en/hqs/fused_silica_quartz_knowledge_base/knowledge_overview/knowlegde_intro.aspx
19. Y. Y. Wang, N. V. Wheeler, F. Couny, P. J. Roberts, and F. Benabid, "Low loss broadband transmission in hypocycloid-core Kagome hollow-core photonic crystal fiber," Opt. Lett. **36** (5), pp. 669-671 (2011).
20. B. Debord, M. Alharbi, T. Bradley, C. Fourcade-Dutin, Y. Y. Wang, L. Vincetti, F. Gérôme, and F. Benabid, "Hypocycloid-shaped hollow-core photonic crystal fiber Part I: Arc curvature effect on confinement loss," Optics Express. **21** (23), pp. 28597-28608 (2013).
21. M. Maurel, M. Chafer, A. Amsanpally, M. Anan, F. Amrani, B. Debord, L. Vincetti, F. Gerome, and F. Benabid, " Optimized inhibited-coupling Kagome fibers at Yb-Nd:Yag (8.5 dB/km) and Ti:Saph (30 dB/km) ranges," Opt. Lett. **43** (7), pp. 1598-1601 (2018).
22. HITRAN database, http://cfa-www.harvard.edu/HITRAN/
23. S. P. Phipps, T. C. Smith, G. D. Hager, M. C. Heaven, J. K. McIver, and W. Rudolph, "Investigation of the state-to-state rotational relaxation rate constants for carbon monoxide (CO) using infrared double resonance," Journal of Chem. Phys. **116**, 9281 (2002).
24. J. J. Olivero, and R. L. Longbothum, "Empirical fits to the Voigt line width: A brief review, " Journal of Quantitative Spectroscopy and Radiative Transfer. **17**, pp. 233-236 (1977).
25. M. Xu, F. Yu, and J. Knight, "Mid-infrared 1 W hollow-core fiber gas laser source," Opt. Lett. **42** (20), pp. 4055-4058 (2017).

Published by OSA® The Optical Society

155.185.104.134 {ts '2020-11-12 09:54:32'}